CHINESE OPTICS LETTERS
Vol. 19, No. 9 | September 2021

Watt-level continuous-wave intracavity frequency-doubled Pr:YLF-LBO laser at 320 nm

Yunshan Zhang (张云杉)[1], Jingyu Zou (邹靖宇)[1], Wanxin Zheng (郑婉馨)[1], Kai Feng (冯 凯)[1], Bin Xu (徐 斌)[1,2*], and Zhenfang Yu (余振芳)[3]

[1] Department of Electronic Engineering, Xiamen University, Xiamen 361005, China

[2] Shenzhen Research Institute, Xiamen University, Shenzhen 518057, China

[3] Analysis and Test Center of Sichuan Province, Chengdu 610000, China

*Corresponding author: xubin@xmu.edu.cn

Received January 20, 2021 | Accepted March 4, 2021 | Posted Online June 3, 2021

We report on diode-pumped continuous-wave Pr-doped yttrium lithium fluoride (Pr:YLF) laser and its frequency doubling to 320 nm. The maximum output power of the 640 nm fundamental wave reached 3.44 W with a slope efficiency of about 48.3%. Using a type-I phase-matched lithium triborate (LBO) crystal as a frequency doubler, we have achieved 320 nm ultraviolet radiation with a maximum output power of 1.01 W, which is the highest power ever reported under diode pumping, to the best of our knowledge.

Keywords: Pr:YLF crystal; frequency doubling; ultraviolet; continuous wave.

DOI: 10.3788/COL202119.091406

1. Introduction

Direct generation of visible lasers has become more and more attractive with the great development of the blue InGaN diode laser. Among the direct visible lasers, researches on diode-pumped Pr^{3+}-doped lasers have gained the greatest success, which can produce green, orange, red, and deep red lasers with high output powers and high efficiencies thanks to the appropriate energy-level scheme of Pr^{3+} ions. The first, to the best of our knowledge, diode-pumped Pr^{3+} laser was been reported in 2004[1]. After this pioneering work, up to now, many Pr^{3+} visible lasers have been demonstrated[2–7]. These directly generated visible lasers have been believed to have advantages in laser efficiency, system compactness, and stability against conventional Nd^{3+} or Yb^{3+} visible lasers via nonlinear frequency conversion.

On the other hand, as we know, the main routes for generating ultraviolet (UV) lasers resort to the third (at about 355 nm[8]) and fourth (at about 266 nm[9]) harmonic generations of Nd^{3+} or Yb^{3+} near-infrared lasers. However, in order to enhance the conversion efficiency, the near-infrared fundamental wave should, in general, be operated in the pulsed mode via *Q*-switching or mode locking. However, for some particular applications in spectroscopy, quantum optics, and bio-photonics[10], UV lasers only in the continuous-wave mode are desired. With respect to this issue, Pr^{3+} ion lasers operating in the visible exhibit great advantages for generating efficient, simple, compact, and more importantly, continuous-wave UV sources via high-efficiency frequency doubling. During the past ten years, several groups have already explored the advantages. In 2006, Richter *et al.*[11] started such investigations by operating a frequency-doubled Pr-doped yttrium lithium fluoride (Pr:YLF) laser for 19 mW UV radiation at 320 nm. It is well-known that the Pr:YLF laser at 640 nm exhibits the highest gain, so we have every reason to believe that a high-power continuous-wave 320 nm laser should be achieved by intracavity frequency doubling of a 640 nm Pr:YLF laser. In 2016, Tanaka *et al.*[12] improved the continuous-wave 320 nm laser to 320 mW at an absorbed power of 3.84 W, which stands for the best achievement ever obtained for this UV radiation.

In order to further explore the potential of this specific UV laser, in this work, using a blue diode laser as the pump source, we have investigated an intracavity frequency doubling of the Pr:YLF laser at 640 nm. Through this research, a watt-level UV 320 nm laser was attained, which represents the best result of the 320 nm UV radiation, to the best of our knowledge.

2. Experimental Setup

A simple and compact laser experimental setup is schematically shown in Fig. 1. The pump source is a beam-reshaped InGaN diode laser with a maximum output power of 12 W. The pump beam waist radius was measured to be about 95 μm after focusing by a 75 mm (focal length) aspheric lens. The laser resonator is a typical V-shaped three-mirror cavity with two flat mirrors (M1 and M3) and a curved mirror (M2, 100 mm

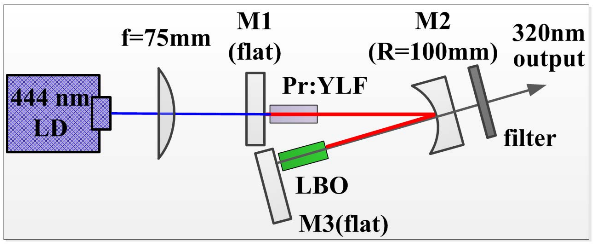

Fig. 1. Laser experimental setup.

curvature radius). The input mirror M1 has a high transmission of about 93% at the pumping wavelength and high reflection of more than 99.9% at 640 nm. The M2 mirror has a high transmission of about 98% at pumping wavelength and high reflection of more than 99.8% at 640 nm. Moreover, the M2 also acted as an output coupler of the UV radiation. It has a high transmission of about 95% at 320 nm. The M3 mirror has a high reflection of more than 99.9% at 640 nm, and it is the second harmonic. In order to compensate the astigmatism due to the curved mirror, we configured the fold angle as small as possible to be about 10°. Note that the three-mirror folded cavity has two separate beam waists: one waist can satisfy the mode-matching condition and the other can enhance the frequency-doubling efficiency.

The laser gain medium is an *a*-cut 0.3% (atomic fraction) doped Pr:YLF crystal with dimensions of $3\,\mathrm{mm}\times 3\,\mathrm{mm}\times 12\,\mathrm{mm}$. In order to mitigate the thermal lensing effect inside the laser crystal, we wrapped it with indium foil and then enclosed it with a copper block. The copper block was water-cooled by a chiller with the temperature set at 12°C. The used linear frequency doubler is a type-I phased-matched ($\theta = 90°$, $\varphi = 53.3°$) lithium triborate (LBO) crystal with dimensions of $3\,\mathrm{mm}\times 3\,\mathrm{mm}\times 12\,\mathrm{mm}$. The optimal operating temperature of the LBO crystal is at room temperature of about 25°C, which was managed by a thermoelectric controller for active temperature control. In addition, both the entrance and the exit surfaces of the LBO are antireflection coated at 640 and 320 nm.

3. Results and Discussion

By optimizing the laser resonator to achieve the highest output power, we configured the V-type cavity with a total physical length of about 188 mm. Under this situation, we plot the stability region of the laser resonator using the standard ABCD matrix, as shown in Fig. 2(a). By shortening the thermal focal length of the laser crystal by increasing the pump power, the laser resonator exhibits an unstable trend, and the present laser configuration could tolerate a short thermal focal length of about −35 mm. Figure 2(b) shows the beam size at different positions of the laser resonator at the full pump power with a rough estimation of the thermal focal length of about −40 mm. The beam waist size was about 100 μm inside the Pr:YLF laser crystal, which was about comparable to the pump beam size. In addition, the beam waist size inside the LBO was also estimated to be about 45 μm. These parameters allow us to estimate the mode overlap efficiency afterwards. It should be pointed out that the astigmatism between the sagittal and tangential beams was almost negligible thanks to the small fold angle.

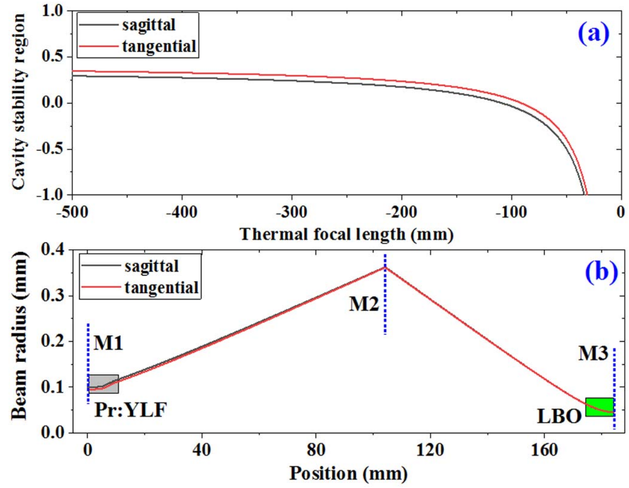

Fig. 2. (a) Cavity stability parameter versus thermal focal length of the laser gain medium; (b) beam sizes at different positions of the laser cavity.

Before operating the UV laser, we carried out the fundamental wave laser operation by replacing the M3 mirror with another flat mirror having a partial transmission of about 4.6% at 640 nm without the insertion of the LBO. Figure 3 shows the output power characteristic. The laser started to oscillate when the absorbed power reached about 0.54 W. Afterwards, the output power almost linearly increased to 3.44 W at a maximum absorbed power of 7.8 W. Thus, we estimated a slope efficiency of about 48.3% of the fundamental wave. We estimate the intracavity round-trip loss L by using the following expression:

$$\eta_s = \frac{\lambda_p}{\lambda_o}\eta_p\eta_e\frac{T}{T+L}, \tag{1}$$

where η_s is the slope efficiency; λ_p and λ_o are the pumping wavelength and laser wavelength, respectively; η_p is the excitation quantum efficiency, which can be assumed to be equal to unity; T is the transmission of the output couplers; L is the intracavity round-trip loss; and η_e is the average mode overlap between the pump beam and the cavity laser beam in the laser crystal, which can be estimated to be about 84%. Substituting the relevant parameter values into this expression, we can calculate the intracavity round-trip loss to be about 1.1%, which indicates a small loss for the present laser.

No rollover can be observed of the laser output power, which indicates a potential for power scaling. We also report the evolution of optical-optical efficiency versus the absorbed power of the 640 nm Pr:YLF laser in the inset of Fig. 3. At the maximum output power, the corresponding optical-optical efficiency is about 44.6%. Moreover, it is clear that with the increase of the absorbed power, the optical-optical efficiency shows an increasing trend, which also indicates good thermal management of the present laser that allows power scaling. We noticed

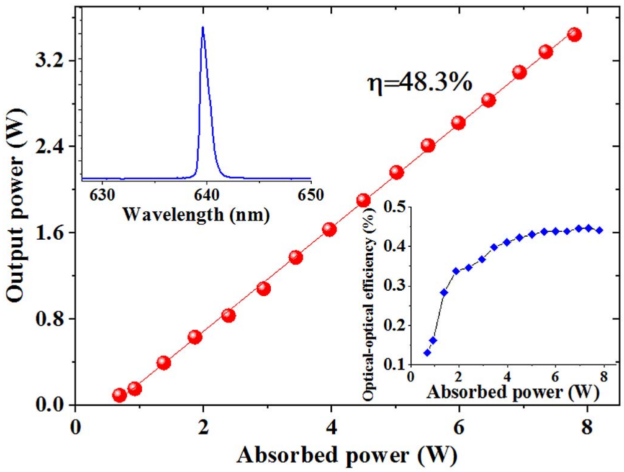

Fig. 3. Output power versus absorbed power of the 640 nm laser; inset: (top-left) laser spectrum and (bottom-right) optical-optical efficiencies.

that the present slope efficiency is a little higher than that reported in Ref. [13] (45.5%), which reported the highest 640 nm Pr:YLF laser (6.7 W) ever achieved to date, to the best of our knowledge. We therefore expect that a higher output power of the 640 nm laser could be achieved by using a higher-power pump source and better thermal management.

An LBO crystal was selected as the frequency doubler because of its small walk-off angle (18.41 mrad), wide spectral ($15.24\,\mathrm{cm}^{-1}\cdot\mathrm{cm}$), angular (2.15 mrad·cm), and temperature (10.05 K·cm) acceptance bandwidths. LBO has a relatively small nonlinear coefficient of 0.544 pm/V; however, it can be compensated for by using a long size, as we used in this work. The LBO crystal was then inserted into the resonator close to the M3 mirror. After a little lengthening of the fold arm and adjustments to the orientation of the LBO, an optimized UV laser operation can be achieved with a maximum output power of 1.01 W, as shown in Fig. 4. The conversion efficiency is about 12.9% with respect to the absorbed power. The UV laser has almost the same

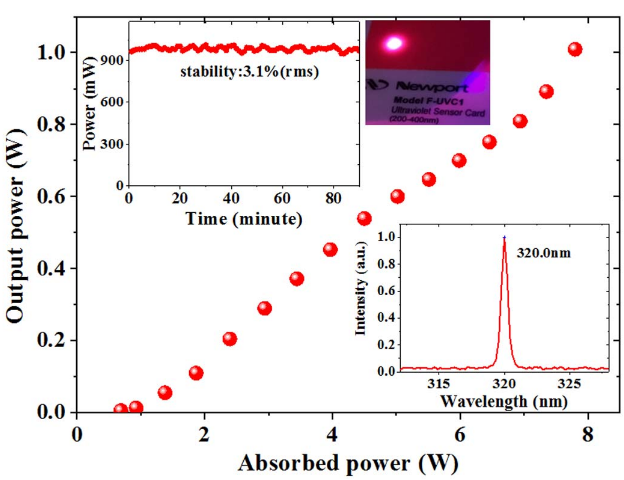

Fig. 4. Output power versus absorbed power of the 320 nm laser; inset: (top-left) output power stability and beam spot on a UV sensor card; (bottom-right) laser spectrum of the 320 laser.

threshold as the fundamental wave, which indicated a low insertion loss arising from the LBO. Compared with the previous result, as reported in Ref. [12], we owe the present high-power output to the usage of a high-power pump source, longer LBO, and relatively weak dopant concentration of the Pr:YLF crystal with good thermal management. In Fig. 4, we show the output beam spot of the UV laser, which was collected by a UV sensor card, from which one can see that the UV showed a circular spot. Unfortunately, we are not able to measure the beam quality because of the lack of a UV CCD for the moment in our lab.

A key factor that affects the stability of the UV laser output power is the temperature of the LBO crystal. In this experiment, we used a Peltier cooler to control the temperature of the LBO. A stable UV laser was obtained by setting the temperature of the LBO crystal at 25°C with precision of 0.05°C. Since the temperature bandwidth of the LBO is 10.05 K·cm, the 0.05°C temperature fluctuation led to good stability of about 3.1% (root mean square) over one and a half hours for the ~1 W UV laser (see in Fig. 4). Using spectrometer (Ocean Insight FLAME), we measured the laser spectrum of the UV, which peaks at 320.0 nm (also see Fig. 4).

4. Conclusion

In conclusion, we achieved a diode-pumped Pr:YLF laser at 640 nm with a maximum output power of 3.44 W and a slope efficiency of about 48.3%. Then, using a type-I phase-matched LBO crystal, we investigated a frequency-doubled Pr:YLF laser at 320 nm with a maximum output power of 1.01 W. It is well known that the Pr:YLF crystal has rich emissions in the visible spectral region besides the red emission. We believe that other violet laser radiations could also be achieved with high-power outputs using a similar laser configuration as reported in this work.

Acknowledgement

This work was supported by the Basic Research Project of Science and Technology Plan of Shenzhen (No. JCYJ20200109105606426) and the Sichuan Science and Technology Program (No. 2021YFSY0028).

References

1. A. Richter, E. Heumann, E. Osiac, G. Huber, W. Seelert, and A. Diening, "Diode pumping of a continuous-wave Pr^{3+}-doped $LiYF_4$ laser," Opt. Lett. **29**, 2638 (2004).
2. P. Camy, J. L. Doualan, R. Moncorgé, J. Bengoechea, and U. Weichmann, "Diode-pumped Pr^{3+}:KY_3F_{10} red laser," Opt. Lett. **32**, 1462 (2007).
3. M. Fibrich, H. Jelínková, J. Šulc, K. Nejezchleb, and V. Škoda, "Visible cw laser emission of GaN-diode pumped Pr:$YAlO_3$ crystal," Appl. Phys. B **97**, 363 (2009).
4. B. Xu, P. Camy, J. L. Doualan, Z. Cai, and R. Moncorgé, "Visible laser operation of Pr^{3+}-doped fluoride crystals pumped by a 469 nm blue laser," Opt. Express **19**, 1191 (2011).
5. B. Xu, F. Starecki, D. Paboeuf, P. Camy, J. L. Doualan, Z. Cai, A. Braud, R. Moncorgé, P. Goldner, and F. Bretenaker, "Red and orange laser operation

of Pr:KYF_4 pumped by a Nd:YAG/LBO laser at 469.1 nm and a InGaN laser diode at 444 nm," Opt. Express **21**, 5567 (2013).
6. M. He, S. Chen, Q. Na, S. Luo, H. Zhu, Y. Li, C. Xu, and D. Fan, "Watt-level Pr^{3+}: YLF deep red laser pumped by a fiber-coupled blue LD module or a single-emitter blue LD," Chin. Opt. Lett. **18**, 011405 (2020).
7. N. Li, J. Huang, B. Xu, Y. Cai, J. Lu, L. Zhan, Z. Luo, H. Xu, Z. Cai, and W. Cai, "Direct generation of an ultrafast vortex beam in a CVD-graphene-based passively mode-locked Pr:$LiYF_4$ visible laser," Photon. Res. **7**, 1209 (2019).
8. Y. Bi, Y. Feng, H. Gong, H. Zhang, and Z. Y. Xu, "High-average power THG of a diode-pumped Nd:YAG laser at 355 nm generated by LiB_3O_5 crystal," Chin. Opt. Lett. **1**, 91 (2003).
9. Q. Liu, X. Yan, M. Gong, H. Liu, G. Zhang, and N. Ye, "High-power 266 nm ultraviolet generation in yttrium aluminum borate," Opt. Lett. **36**, 2653 (2011).
10. T. Gun, P. Metz, and G. Huber, "Efficient continuous wave deep ultraviolet Pr^{3+}:$LiYF_4$ laser at 261.3 nm," Appl. Phys. Lett. **99**, 181103 (2011).
11. A. Richter, N. Pavel, E. Heumann, G. Huber, D. Parisi, A. Toncelli, M. Tonelli, A. Diening, and W. Seelert, "Continuous-wave ultraviolet generation at 320 nm by intracavity frequency doubling of red-emitting praseodymium lasers," Opt. Express **14**, 3282 (2006).
12. H. Tanaka, R. Kariyama, K. Iijima, and F. Kannari, "50-kHz, 50-ns UV pulse generation by diode-pumped frequency doubling Pr^{3+}:YLF *Q*-switch laser with a Cr^{4+}:YAG saturable absorber," Appl. Opt. **55**, 6193 (2016).
13. H. Tanaka, S. Fujita, and F. Kannari, "High-power visibly emitting Pr^{3+}:YLF laser end pumped by single-emitter or fiber-coupled GaN blue laser diodes," Appl. Opt. **57**, 5923 (2018).